Full-Scale 3D Numerical and Laboratory Simulations of Glaze Ice Accretion on a Non-Energized Station Post Insulator

W.J. Rudzinski, M. Farzaneh* and E.P. Lozowski

Department of Earth and Atmospheric Sciences, University of Alberta
Edmonton, Alberta, Canada, T6G 2E3
wjr@ualberta.ca, Edward.Lozowski@ualberta.ca

*NSERC/Hydro-Quebec/UQAC Industrial Chair on Atmospheric Icing of Power Network Equipment (CIGELE) and Canada Research Chair on Engineering of Power Network Atmospheric Icing (INGIVRE), Université du Québec à Chicoutimi
Chicoutimi, Québec, Canada, G7H 2B1
farzaneh@uqac.uquebec.ca

* Chairholder of CIGELE / INGIVRE

***Abstract*— Numerical and laboratory simulations of ice accretion on a standard porcelain post insulator were investigated. A novel, high-resolution, full-scale 3D discrete particle model for glaze ice accretion on a non-energized industrial standard station post insulator was developed. The model is capable of predicting the ice accretion mass and its detailed distribution over the structure under a range of glaze icing conditions. The 3D computer simulations of ice accretion are examined as a function of the microscopic model parameters. In order to validate the model, a series of laboratory experiments has been undertaken at the CIGELE Precipitation Icing Simulation Laboratory at the Université du Québec à Chicoutimi. The influence of ambient conditions on the mass and dimensions of the ice accretion has been investigated. A quantitative comparison between model predictions and experiments has been made, and a relationship between the model parameters and atmospheric variables has been derived.**

Keywords: Freezing precipitation, ice accretion, icing model, icicles, flashover, high-voltage insulator.

I. Introduction

There have been numerous reports of power failure in cold climate countries due to ice accumulation on high voltage insulators [1]-[4]. Ice accretion on an outdoor insulator can cause a considerable decrease in its dielectric performance. Glaze ice with icicles, formed during freezing precipitation, is the most severe type of ice accretion for insulators [5]. When icicles bridge shed spacings and unfrozen or melt liquid flows along the accretion surface, the leakage distance of the insulator may be reduced to the point where it becomes susceptible to electrical discharges and flashover occurrences [6]. Consequently, in an engineering context, it is important to understand glaze ice build-up in order to develop a strategy to reduce or prevent flashover occurrences.

Studying ice accretion on insulators can be undertaken with field and laboratory investigations, as well as by mathematical modelling. Field studies are obviously limited to the Winter season. Laboratory experiments, on the other hand, can be conducted without interruption due to seasonal changes, and with more precise control of the atmospheric conditions. However, they are costly and time consuming, and they cannot perfectly reproduce natural conditions. The advantage of mathematical modelling lies in its flexibility to simulate a variety of meteorological conditions, including the rare extreme conditions, and to predict the morphology and structure of ice accretions at reasonable cost and in a relatively short period of time. Numerical models can be validated using a reduced number of laboratory experiments and field measurements, thereby effecting a substantial saving in money, time and effort.

Over the past five decades, numerous theoretical models have been formulated to simulate ice accretion on various structures. Most of these models employ a classical approach (also referred to as the "Messinger method"), based on continuous partial differential equations applied to a control volume. They have been successfully applied to icing on objects of simple geometry such as power transmission conductors [7]. In the case of insulators, the complexity of their shapes, with numerous sheds, and the complexity of the ice accretion shape, with numerous icicles, has precluded the application of such traditional models. In order to deal with this complexity of ice accretion morphology, stochastic discrete particle models have recently been developed [8], [9]. They are also referred to as "morphogenetic models".

Morphogenetic models have their roots in cellular automata and discrete particle methods [10]. They emulate the growth of an ice accretion under a flowing liquid film by considering the Lagrangian behavior of individual fluid particles which undergo a quasi-random walk through a geometrical lattice. They can be categorised according to the degree of mobility that is accorded to the fluid particles following impact with the

structure or the existing ice accretion [11]. In the present model, we allow unlimited droplet movement over the structure, the principal constraints being that the particles are not permitted to "walk" away from or into the surface of the accretion and their predominant motion is dictated by wind stress and gravity. Szilder [12], [13] and Szilder and Lozowski [14], [15] were the first to introduce such an approach to the modelling of ice accretion. Among other things, they simulated ice accretion at a reduced scale on a hemisphere representing a single insulator shed, under freezing rain conditions, with vertical raindrop trajectories. In a morphogenetic model, the shape of the ice accretion is determined by the motion of fluid particles and their freezing on the structure. A significant advantage of morphogenetic models as applied to insulator icing is their ability to simulate icicle formation.

The objective of this paper is to introduce, test and validate by laboratory experiments a full-scale 3D discrete particle model for predicting the glaze ice accretion on a non-energized industrial standard station post insulator. The scope of the paper is as follows. In Section II, the model principles and present results of sensitivity tests are introduced. In Section III, the laboratory experiments and experimental results are described. In Section IV, a quantitative comparison of the numerical simulations with the icing experiments as a part of model validation are made. Finally, the paper is concluded and recommendations for future research are offered.

II. Numerical Simulations

A. High Resolution Model

The model consists of two parts: a particle trajectory model and a random walk model. The particle trajectory model determines the initial impact location of a particle, while the random walk model predicts its motion along the surface of the substrate, which consists of the insulator and any ice already formed on it. The simulation domain is a rectangular prism, consisting of 350 x 350 x 2500 cubic elements in a three-dimensional lattice with 1 mm resolution. One at a time, particles are fired at the model insulator with a height of 1540 mm, a shed diameter of 262 mm, and a flange diameter of 288 mm, that is centered in the domain. The particle trajectories are straight lines, with a fixed angle to the vertical. The trajectory starting points are randomly chosen locations on a 350 mm x 2500 mm vertical plane that constitutes one of the vertical faces of the domain. The model wind direction is, by implication, perpendicular to this face and blowing into the domain. The angle of particle impingement can be varied in the model, but in the present simulations, a constant angle of 45 degrees is used. These assumptions about particle trajectories are consistent with freezing rain with a monodisperse drop distribution. The large inertia and uniform size of the drops will insure that there is a little deviation of the trajectories from straight lines.

A particle is considered to collide with the substrate if it reaches a lattice cell which is in corner, edge or face contact with a lattice cell already occupied by ice or by an insulator element. From the point of impact, the particle begins a random walk over the structure. The random walk of the particle consists of a series of stochastic moves through the unoccupied cells of the lattice. Since the model is 3D, at each step along a particle's path, it encounters eight possibilities: the particle may move one cell downwind or upwind, left or right (relative to the downwind direction) or down (up is not allowed), it may freeze "in situ", it may drip or it may remain in place. Upward motion and diagonal motion are not allowed during a particle's random walk. The term "step" used here refers to the process that consists of generating a pseudo-random number (with a uniform distribution between 0 and 1), and using the number to determine what a particle does next. As mentioned above, there are eight possible particle transitions. A probability is specified for each of the first six particle transitions, namely, freezing or translation by one cell in the lattice. The actual outcome for the particle is determined by the value of the generated random number. The sum of the probabilities of all six transitions is unity, each being assigned its own range within the interval 0 to 1.

A particle is prohibited from moving away from the surface, being required to maintain corner, edge or face contact with the existing surface. Particles are also prohibited from moving into the ice accretion that is from trying to occupy an already occupied cell. If, as a result of the random draw, a particle attempts to make such a forbidden move, it is forced to remain in place until the next step.

In an attempt to allow for the effect of wind stress on particle motion, it is assumed that the ratio of the difference between the probabilities of horizontal motion downwind and upwind, to the probability of downward motion is unity. This ratio is called the "motion parameter". Our selected value for the motion parameter, namely 1.0, is based on an order of magnitude analysis of the forces acting on an isolated particle in a wind field and a gravitational field [11].

A particle is allowed to move along the surface indefinitely, unless its random walk is terminated in some way. This may happen in one of two ways. The first is by freezing. If freezing is determined to occur, by random draw, the particle does not simply remain in its current cell. Instead, a cradle location is sought for the "frozen" particle in the neighbourhood of its present cell. This neighbourhood is defined as a cube whose edge length, in cells, is called the "freezing range parameter". In the present simulations, the freezing range parameter is taken to be 5. The "frozen" particle is moved to the empty cell in this cube where it will have the maximum number of occupied neighbours. If there is more than one such location, the final location is chosen randomly from among them. The purpose of the cradle location search is to perform something akin to numerical "annealing" of the ice structure. This has the effect of making it more compact, with a view to minimizing the occurrence of voids and achieving an ice density in line with the relatively high values typically observed during freezing precipitation.

The other way to end a particle's random walk, either temporarily or permanently, is to let it drip from the structure. This is allowed to happen in the model only when a particle reaches a local minimum level on the insulator or the ice structure. If a particle remains at such a level without freezing, for more steps than a critical value called the shedding

parameter, it is forced to drip from that part of the structure. Thereafter, it follows a vertical straight line trajectory downward. For dripping particles, vertical trajectories were chosen, rather than 45 degrees trajectories, in part because they are algorithmically easier to implement, and in part because we would expect shed drops to fall more vertically than the originally impinging drops. If a falling particle re-impinges upon the insulator or ice accretion lower down, its random walk is continued. Re-impingement occurs if the dripped particle collides again with a lower part of the insulator or ice accretion. However, the particle's random walk is terminated permanently if the particle does not re-impinge the insulator or the ice accretion structure after dripping, i.e. if it passes through the lower boundary of the domain. Particles passing through the lower boundary of the domain are counted as part of the permanently shed water mass.

The freezing probability and the shedding parameter are expected to be functions of the atmospheric conditions, including air temperature, wind speed and precipitation rate. For a single conical icicle, these functions have been estimated by Szilder and Lozowski [14], using a simple analytical approach based on energy and mass conservation. The relations are expected to be more complex for insulator icing, and no theory currently exists to determine them. Consequently, we have proceeded empirically by comparing the results of 3D simulations with 3D laboratory experiments.

In the case of energized insulators, in addition to the environmental variables listed above, several other factors related to corona discharge, ionic wind, the heating effect of local arcs, especially near electrodes, as well as the geometrical and electrical characteristics of the insulator also intervene [6], [16]. However, because of the complexity of the subject, only the modelling of a non-energized insulator will be considered, for now.

In the next subsection, the results of 3D numerical simulations of ice accretion on a full-scale station post insulator will be presented. In particular, the sensitivity of the ice accretion mass and dimensions to variations in the model's microscopic parameters, specifically the freezing probability and the shedding parameter, will be examined.

B. Simulation Results

The 3D simulations of ice accretion on a full-scale insulator were performed on the WestGrid supercomputers Nexus and Arcturus, over a wide range of model parameters, especially the freezing probability and the shedding parameter (Table 1). As shown in the table, the freezing probability was varied from 0.001 % to 0.1 %, the shedding parameter from 100 to 3000, the motion parameter was set to 1, the freezing range parameter 5, and the angle of particle impingement 45 degrees to the vertical.

In all simulations, the total precipitation was either 0.5, 1.0, 2.0 or 4.0 mm. These values are much lower than the "standard" value of 27 mm, which was used in the experiments (see Section III). Lower values of total precipitation were chosen, of necessity, in order to reduce computation time, since it was not practical to exceed 24 hours of wall time for a single simulation and because we were constrained to run the code on a single processor. We were therefore left with the dilemma of how to compare numerical simulations with relatively low precipitation, with experiments where the total precipitation was considerably higher, at least in some cases. In order to do this, it was attempted to establish relationships between the total mass and mass distribution of the ice accretion and the total precipitation. For each simulation, the mass of ice and the mass distribution parameters were determined at the end of four successive intervals, each with the same precipitation. In general, the behaviour of the mass and the mass distribution parameters with increasing precipitation was essentially linear (Fig.1). On this basis, it was concluded that a linear extrapolation to higher precipitation amounts could be justified. The mass distribution parameters are specified as: the average icicle number per insulator shed, the average icicle thickness measured at halfway point between two adjacent sheds, the average icicle length formed at the top and bottom of the insulator, the average icicle spacing, and the average extent of the icicle zone around the shed perimeter. The averages are taken over the entire insulator.

TABLE 1
NUMERICAL SIMULATION CONDITIONS.

Run #	Freezing Probability (%)	Shedding Parameter	Total Precipitation (mm)
1	0.1	3000	4.0
2	0.1	1000	4.0
3	0.1	300	4.0
4	0.1	100	4.0
5	0.03	3000	4.0
6	0.03	1000	4.0
7	0.03	300	4.0
8	0.03	100	4.0
9	0.01	3000	2.0
10	0.01	1000	2.0
11	0.01	300	2.0
12	0.01	100	2.0
13	0.003	3000	1.0
14	0.003	1000	1.0
15	0.003	300	1.0
16	0.003	100	1.0
17	0.001	3000	0.5
18	0.001	1000	0.5
19	0.001	300	0.5
20	0.001	100	0.5

An example of the simulated ice accretion on a model station post insulator is shown in Fig. 2. The numerical experiment was carried out under the following conditions: total precipitation 4 mm, freezing probability 0.03 %, motion parameter 1, freezing range parameter 5, shedding parameter 1000, and angle of particle impingement 45 degrees to the vertical. The ice is formed primarily on the upwind side of the insulator. Long icicles develop at the top and bottom of the insulator, while shorter ones bridge the gaps between the insulator sheds. Both the longer and shorter icicles are inclined downwind. The morphology of this example is qualitatively similar to that of all ice accretions simulated under the present range of numerical conditions. Quantitative

differences are observed in the overall mass of the ice accretion, the number of icicles per shed, their thickness, length, spacing and extent around the shed perimeter.

Fig. 3 shows the relation between the total mass of ice and the freezing probability. Based on a linear relationship between the total mass of ice and the total precipitation, the total mass of ice was extrapolated to the "standard" experimental amount of 27 mm.

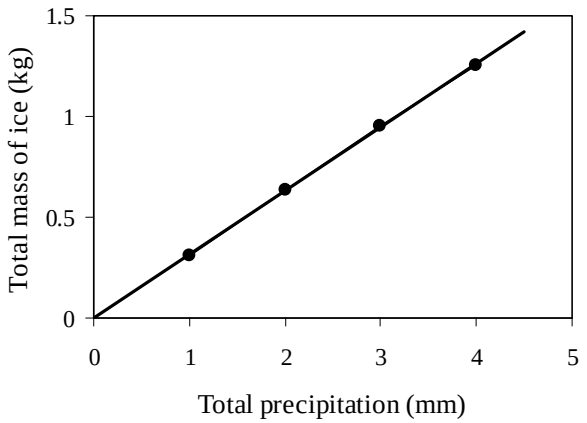

Fig. 1. Relationship between total mass of ice and total precipitation. The freezing probability is 0.03 %, shedding parameter 1000, motion parameter 1, freezing range parameter 5, and angle of particle impingement 45 degrees to the vertical.

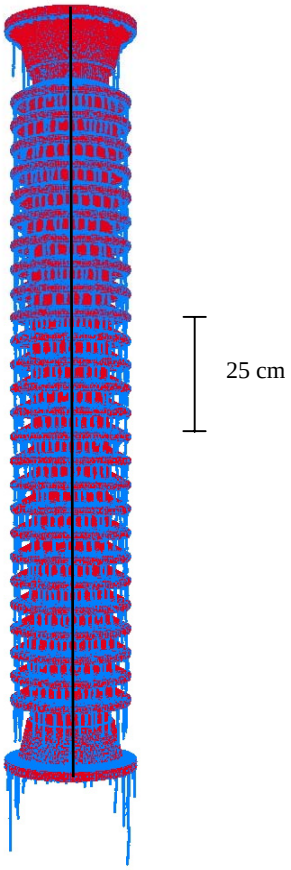

Fig. 2. Simulated ice accretion (blue) resulting from freezing rain on a station post insulator (red). The total precipitation is 4 mm. The other conditions are the same as in Fig.1. The black vertical line represents the stagnation line of the air flow around the insulator.

In all cases, as the freezing probability increases from its lowest value (0.001%), the mass of ice increases until it reaches a saturation level of about 11 kg. This saturation level corresponds to the condition in which all the impinging droplets freeze somewhere on the structure. Over the range of simulated conditions, the accretion mass also increases with increasing shedding parameter. Fig. 4 shows the relation between the accretion mass and the shedding parameter, for five values of the freezing probability. This effect may be explained as follows. A higher value of the shedding parameter means that fluid particles remain longer at the local minimum level prior to dripping. Hence they are more likely to freeze there. The shedding parameter appears to have the greatest influence on accretion mass for intermediate values of freezing probability.

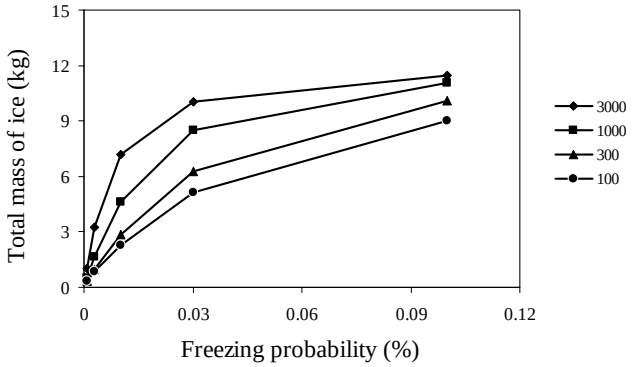

Fig. 3. Influence of freezing probability on the total mass of the ice accretion. The total precipitation is 27 mm. The other conditions are the same as in Fig.1. The curves are for different values of the shedding parameter.

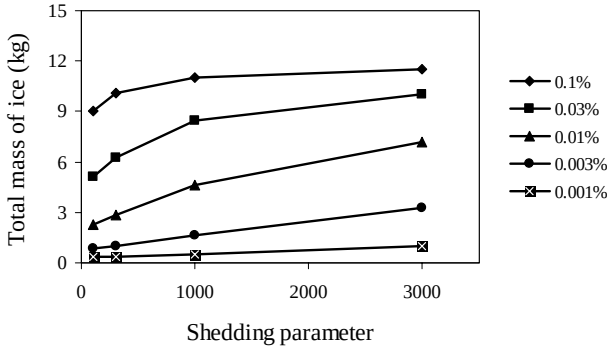

Fig. 4. Influence of shedding parameter on the total mass of the ice accretion. The total precipitation is 27 mm. The other conditions are the same as in Fig.1. The curves are for different values of the freezing probability.

Fig. 5 shows the influence of freezing probability on the average icicle length at the top and the bottom of the insulator on the upwind side along the stagnation line. There is a linear increase in the icicle length as the freezing probability increases. This relation can be approximated by a straight line through the origin with a slope of 1.3×10^3 mm $(\%)^{-1}$.

III. Laboratory Experiments

A. Experimental Facility, Set up and Icing Conditions

In order to validate and calibrate the model, laboratory investigations of insulator icing were undertaken in the Precipitation Icing Simulation Laboratory of the Industrial Chair on Atmospheric Icing of Power Network Equipment (CIGELE) at the Université du Québec à Chicoutimi. The experiments were carried out in the vertical circulation cold room (6m x 6m x 9m). A non-energized 735 kV industrial standard station post insulator with 26 sheds was sprayed for 30 minutes (in some cases for 120 minutes) using six air-atomizing nozzles mounted on a vertical support parallel to the axis of the insulator. In order to try to achieve a uniform ice accretion on the insulator surface, the nozzles were oscillated in a vertical plane from 0 to 45 degrees below horizontal. The nozzles were fed with de-ionized water at outside room temperature. Because of cooling in the feed lines and in the air, the temperature of the water droplets impinging on the insulator was estimated to be very close to the cold room air temperature. Wind was generated by fans placed in a tapered box (similar to a wind tunnel contraction), with a honeycomb panel behind the nozzles to straighten the flow and reduce the scale of turbulence. A set of fixed louvers, installed between the nozzles and the flow contraction box, directed the air flow at 45 degrees to the horizontal.

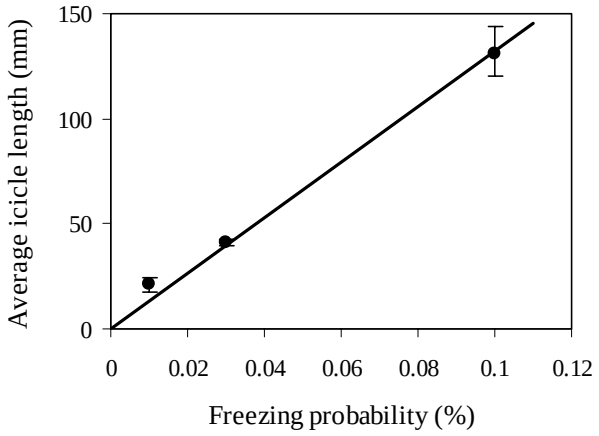

Fig. 5. Influence of freezing probability on average icicle length along the stagnation line at the top and the bottom of the insulator. The total precipitation is 27 mm. The other conditions are the same as in Fig. 1. The error bars represent extreme values.

The experiments were carried out under the following atmospheric conditions (where the underlined values correspond to "standard conditions"`): air temperature -12, -6, -4 and -3 °C; wind speed 3.5 and 5.7 m s^{-1}, precipitation rate 4, 11, 39 and 54 mm h^{-1}; median volume diameter (MVD) of droplets 0.14 and 0.31 mm. The cold room temperature was controlled with a precision of ± 1°C by a proportional integral differential system, and was measured with a thermistor mounted at mid-height in the cold room. The wind speed was measured near the stagnation line at the top, bottom and middle of the insulator using a hand-held propeller anemometer, oriented perpendicular to the overall mean flow. The precipitation rate and droplet size distribution were controlled by the water and air pressure and water flow rate applied to the nozzles. The precipitation rate was measured near the stagnation line of the insulator with a Hydro-Québec designed pluviometer. The median volume diameter of the droplets was estimated using oiled slides exposed to the spray. The slides were examined under a microscope and approximately 1000 droplets were counted to determine the size distribution for each experiment. Ice sponginess was measured using a specially designed calorimeter [17]. The total mass of ice on the insulator was determined following the icing experiment, by collecting and measuring the volume of the meltwater. Digital photography was used to record the shape of the ice accretion. A total of more than 2000 photographs were taken during 22 successful experiments (Table 2).

B. Experimental Results

Fig. 6 shows the station post insulator covered with glaze ice grown under the following conditions: air temperature -6 °C, wind speed 5.7 ms^{-1}, precipitation rate 54 mm h^{-1}, and MVD 0.31 mm. The ice accretion grew primarily on the upwind side of the insulator. Long icicles are formed at the top and bottom of the insulator, while shorter ones bridge the gaps between the insulator sheds. Most of the icicles are inclined downwind. The shape of this example is qualitatively similar to that of all glaze ice accretions grown under the present range of experimental conditions. Quantitative differences are observed in the number of icicles per shed, their thickness and length, their inclination angle to the vertical, their distribution along the shed, and the overall mass of the ice accretion.

TABLE. 2
EXPERIMENTAL ICING CONDITIONS.

Expt. #	Temp. (°C)	Wind (ms^{-1})	Ppn. (mm)	MVD (mm)	Ice Type
1	-12.	5.7	27.	0.31	Glaze
2	-12.	5.7	27.	0.31	Glaze
3	-12.	5.7	27.	0.31	Glaze
4	-6.	5.7	27.	0.31	Glaze
5	-12.	3.5	27.	0.31	Glaze
6	-6.	3.5	27.	0.31	Glaze
7	-6.	5.7	27.	0.31	Glaze
8	-6.	3.5	27.	0.31	Glaze
9	-6.	5.7	19.5	0.14	Glaze
10	-4.	5.7	27.	0.31	Glaze
11	-6.	3.5	19.5	0.14	Glaze
12	-12.	3.5	19.5	0.14	Rime
13	-3.	5.7	19.5	0.14	Glaze
14	-6.	5.7	22.	0.31	Rime
15	-3.	5.7	22.	0.31	Glaze
16	-3.	3.5	22.	0.31	Glaze
17	-6.	3.5	8.	0.14	Rime
18	-3.	5.7	8.	0.14	Rime
19	-3.	3.5	8.	0.14	Rime
20	-6.	5.7	135.	0.31	Glaze
21	-12.	5.7	54.	0.31	Glaze
22	-3.	3.5	78.	0.14	Glaze

Fig. 7 shows the experimental relationship between the total mass of ice and total precipitation. The mass of the ice accretion increases linearly with increasing total precipitation. This function can be approximated by a straight line through the origin with a slope of 0.16 kg mm^{-1}. This value differs from the slope of the simulations in Fig. 1 because the conditions are not equivalent. However, the linear behaviour inferred from Fig. 1 is confirmed, experimentally.

Fig. 8 shows the relationship between the total mass of the ice accretion and air temperature. The mass of the ice accretion increases with decreasing temperature. This relationship is characterized by a linear trend from the freezing point to -12 °C with a slope of -0.44 kg $°C^{-1}$ and an intercept of 1.0 kg. The intercept could represent a residual unfrozen liquid film in the experiments. Or possibly, it means that the relation is not perfectly linear. In any event, the behaviour cannot remain linear as the temperature continues to fall, since the total mass must reach an asymptotic limit. Repeated measurements showed that the change in the mass of ice between "identical" experiments did not exceed 15%.

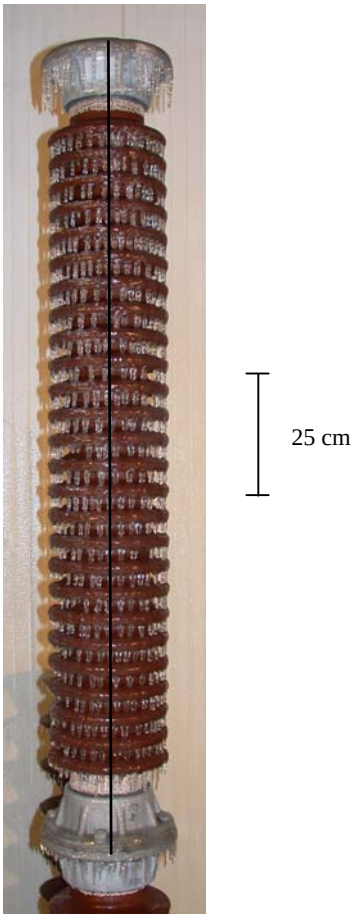

Fig. 6. Station post insulator covered with glaze ice. The conditions of the experiment were: air temperature -6 °C, wind speed 5.7 ms^{-1}, total precipitation 27 mm, MVD 0.31 mm. The black vertical line represents the stagnation line of the flow around the insulator.

Fig. 9 shows the influence of air temperature on the average icicle length at the top and bottom of the insulator on the upwind side along the stagnation line. As the air temperature increases from -12 °C, the average icicle length decreases almost linearly. This relation can be approximated by a straight line through the origin with a slope of -14.0 mm $°C^{-1}$. This is similar to the variation of icicle length with freezing probability in the simulations.

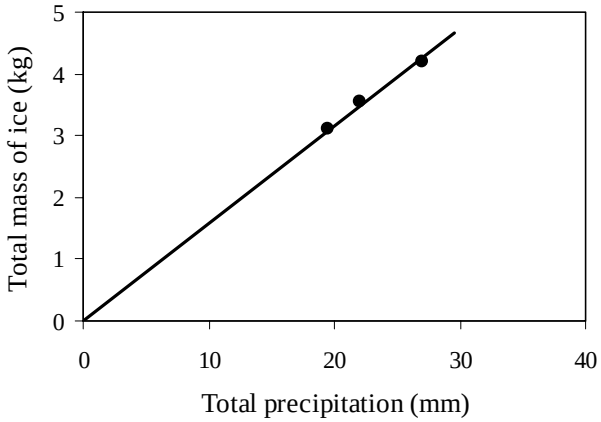

Fig. 7. Relationship between total mass of ice and total precipitation. The other conditions are the same as in Fig. 6.

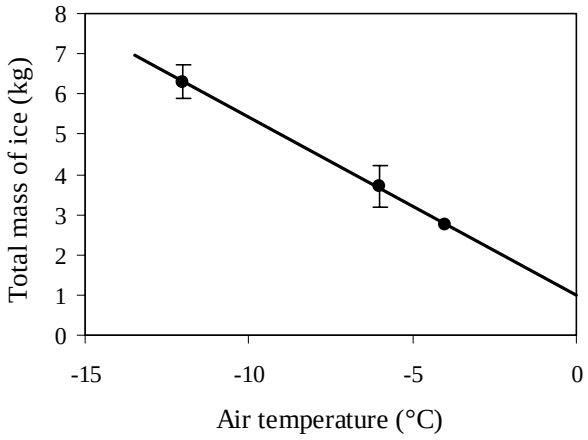

Fig. 8. Influence of air temperature on the total mass of ice. The other conditions are the same as in Fig. 6. The error bars represent extreme values, while the points are averages of several experiments conducted under the same conditions. There was only one experiment conducted at -4 °C, hence there is no error bar.

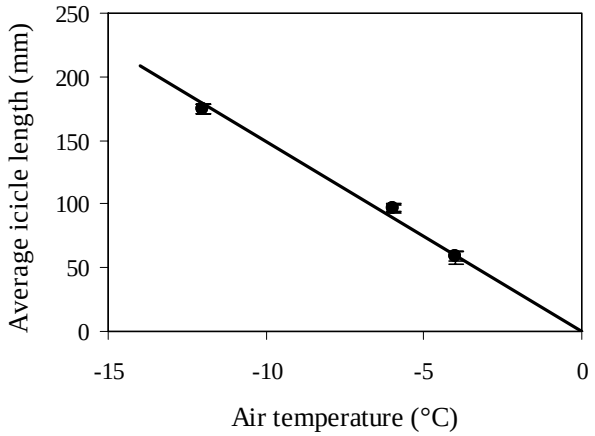

Fig. 9. Influence of air temperature on average icicle length along the stagnation line at the top and the bottom of the insulator. The other conditions are the same as in Fig. 6. The outer error bars represent extreme values, while the inner bars are standard deviations.

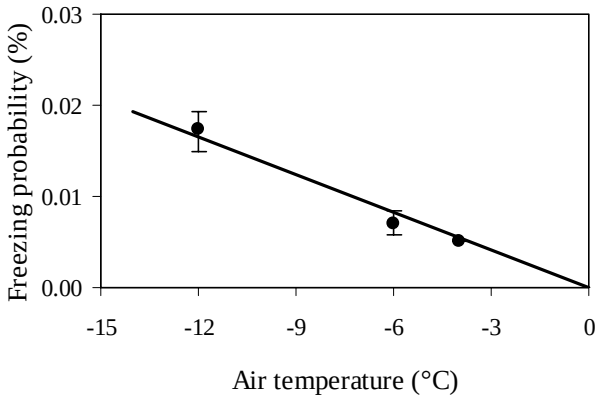

Fig. 10. Relationship between freezing probability and air temperature for a shedding parameter of 1000. The error bars represent extreme values, while the points are averages of several experiments conducted under the same conditions. There was only one experiment conducted at -4 °C, hence there is no error bar.

IV. Discussion

Both the numerical simulations and experiments exhibited linear trends relating ice accretion mass and total precipitation. Over a range of simulation parameters, the ice mass growth rate per unit of precipitation varied from 0.01 to 0.42 kg mm^{-1}. The experiments conducted under standard conditions showed a growth rate of 0.16 kg mm^{-1} at -6 °C and 0.22 kg mm^{-1} at -12 °C.

In both model and experiment, the ice accretion mass increases with increasing freezing probability (in the simulations) and airstream supercooling (in the experiments). Since both freezing probability and airstream supercooling should be related to external heat transfer with the airstream, it appears that the simulations are exhibiting similar trends to the experiments. In order to establish a relationship between the freezing probability and air temperature, an empirical approach was applied, based on a comparison of the total mass of ice for a series of laboratory experiments and corresponding numerical simulations. By comparing the relation between the total mass of ice and air temperature in the experiments with the relation between the total mass of ice and the freezing probability in the simulations under the same total precipitation, a relation between the freezing probability and air temperature was derived (Fig. 10).

As shown in Fig. 10, the freezing probability decreases linearly with increasing air temperature. This relation can be approximated by a straight line through the origin with a slope of -1.4 x 10^{-3} (%) °C^{-1}.

In both numerical simulations and experiments, the ice accretion dimensions increase with increasing freezing probability (in the simulations) and airstream supercooling (in the experiments). The average icicle length along the stagnation line at the top and bottom of the insulator is comparable and increases linearly with increasing freezing probability and decreasing air temperature.

Another remarkable feature of the model is its ability to predict the quantitative behaviour of the icicle inclination angle. In the experiments, as the wind speed increases from 3.5 to 5.7 m s^{-1}, the average inclination angle (to the vertical) of the top and bottom icicles increases from 3.5 to 13.0 degrees [18]. In the simulations, the average inclination angle of the top and bottom icicles is almost identical to that observed in the cold room at the higher wind speed.

V. Conclusions and Recommendations

Theoretical predictions of the mass and morphology of the ice accretion on a non-energized station post insulator are in qualitative agreement with experimental results. Steps have also been taken to make this agreement quantitative as well. The high resolution full-scale 3D model is capable of predicting the shape, mass and dimensions of the ice accretion on a station post insulator. The quantitative comparison of the mass of the ice accretion between simulations and experiments has led to establishing a relationship between the model parameter, freezing probability and air temperature.

In order to complete the validation of the present model, further quantitative comparisons of the ice accretion mass distribution parameters, such as the average icicle number per insulator shed, icicle thickness, icicle spacing, and the extent of the icicle zone around the shed perimeter need to be made.

VI. Acknowledgments

The authors are grateful for a research grant from the Canadian Foundation for Climate and Atmospheric Sciences.

VII. References

[1] M. Kawai, "AC flashover test at project UHV on ice-coated insulators," *IEEE Transactions on Power Apparatus & Systems*, PAS-89, pp.1800-1804, 1970.

[2] M.D. Charneski, G.L. Gaibrois, and B.F. Whitney, "Flashover tests on the surface of conductive ice," *IEEE Transactions on Power Apparatus & Systems*, PAS-101, pp. 2429-2433, 1982.

[3] O.T. Melo, Y.T. Tam and M. Farzaneh, "Freezing rain and fog events in southern Ontario," in *Proc. 1988 4th International Workshop on Atmospheric Icing on Structures*, pp. 70-75.

[4] M. Farzaneh and J.F. Drapeau, "AC flashover performance on insulators covered with artificial ice," *IEEE Transactions on Power Delivery*, vol.10, pp. 1038-1051, 1995.

[5] M.Farzaneh and K. Kiernicki, "Flashover performance of IEEE standard insulator under ice conditions," *IEEE Transactions on Power Delivery*, vol. 12, pp. 1602-1613, 1997.

[6] M.Farzaneh, "Ice accretion on high-voltage conductors and insulators and related phenomena," *Philosophical Transactions of the Royal Society, London*, vol. 358, pp. 2971-3005, 2000.

[7] G. Poots, *Ice and Snow Accretion on Structures*, New York: Research Studies Press Ltd. John Wiley & Sons Inc., 1996, p. 338.

[8] E.P. Lozowski, K. Szilder and L. Makkonen, "Computer simulation of marine ice accretion,"*Philosophical Transactions of the Royal Society, London*, vol. 358, pp. 2811-2845, 2000.

[9] K. Szilder, E.P. Lozowski and M. Farzaneh, "Morphogenetic modelling of wet ice accretion on transmission lines as a result of freezing rain," *International Journal of Offshore and Polar Engineering*, vol. 11, pp. 6-22, 2001.

[10] H. Chen, C. Teixeira and K. Molvig, "Digital physics approach to computational fluid dynamics: some basic theoretical features," *International Journal of Modern Physics*, C, vol.8, pp. 675-684, 1997.

[11] W. Rudzinski, "Numerical and experimental modelling of ice accretion on a non-energized station post insulator under freezing rain conditions," Ph.D. dissertation, Dept. Earth and Atmospheric Sci. Univ. of Alberta, Edmonton, in preparation, 2005.

[12] K. Szilder, "The density and structure of ice accretion predicted by a random walk model," *Quarterly Journal of the Royal Meteorological Society*, vol.119, pp. 907-924, 1993.

[13] K. Szilder, "Simulation of ice accretion on a cylinder due to freezing rain," *Journal of Glaciology*, vol.40, pp. 586-594, 1994.

[14] K. Szilder and E.P. Lozowski, "Stochastic modelling of icicle formation,"*Journal of Offshore Mechanics and Arctic Engineering*, vol. 116, pp. 180-184, 1994.

[15] K. Szilder and E.P. Lozowski, A new method of modeling ice accretion on objects of complex geometry," *International Journal of Offshore and Polar Engineering*, vol.5, pp. 37-42, 1995.

[16] M. Farzaneh and J.L. Laforte, "Effect of voltage polarity on icicles growth on line insulators," *International Journal of Offshore and Polar Engineering*, vol.2, pp. 241-246, 1992.

[17] R. Z. Blackmore, E.P. Lozowski and M. Farzaneh. "A portable calorimeter for measuring liquid fraction of spongy freshwater ice accretions," in *Proc. 17th IAHR International Symposium on Ice*, vol.1, pp. 393-399, 2004.

[18] W. J. Rudzinski, E. P. Lozowski and M. Farzaneh. "A qualitative comparison of icing experiments with a high resolution full-scale 2D model of glaze ice accretion on a non-energized station post insulator," in *Proc. 13th International Offshore and Polar Engineering Conference*, (CD), pp. 416-422, 2003.